Introduction to Electrocatalysis

John T. S. Irvine[a]

[a]University of St Andrews, School of Chemistry, Purdie Building, KY16 9ST, St. Andrews, UK
*E-mail: jtsi@st-and.ac.uk

13.1 Introduction

Electrochemical devices function *via* the transport of ions between two electrodes through an electrolyte, in parallel with the transport of electrons through an electronic circuit. The underlying electrochemistry that determines the efficacy of the device involves the transfer of charge at the electrodes. Typically, the electrochemical reactions are associated with a barrier to charge transfer that is termed the overpotential, electrocatalysis can reduce this barrier to charge transfer.

Electrochemical systems are largely classified by the constituent phases in the active elements. The electrolyte is a phase that allows the transport of ions and blocks the transport of electrons, this would be considered as an ionic transport number of unity. Most commonly lectrolyte is a solution under ambient conditions with an ionic salt, acid or base dissolved in a polar solvent such as water or propylene carbonate. There are also important examples where the electrolyte is a ceramic or polymer or molten salt/ionic liquid.

Contemporary Catalysis: Science, Technology, and Applications
Edited by Paul C. J. Kamer, Dieter Vogt and Joris W. Thybaut

Published by the Royal Society of Chemistry, www.rsc.org

At the electrodes in an electrochemical cell, either an oxidation or a reduction reaction occurs conserving both ions and electrons across the whole cell, as shown in the following.

13.1.1 Cathode – Reduction

$$X + ne^- \rightarrow X^{n-} \tag{13.1}$$

$$\textit{e.g.}\text{ in fuel cell: } O_2 + 4e^- \rightarrow 2O^{2-} \tag{13.2}$$

13.1.2 Anode – Oxidation

$$M \rightarrow M^{n+} + ne^- \tag{13.3}$$

$$\textit{e.g.}\text{ in fuel cell: } H_2 \rightarrow 2H^+ + 2e^- \tag{13.4}$$

A typical example is the copper zinc-based Daniel cell.

$$Cu_{(aq)}{}^{2+} + Zn_{(s)} \Leftrightarrow Cu_{(s)} + Zn_{(aq)}{}^{2+} \tag{13.5}$$

Within an electrochemical device, there are two types of current flow:

1. Faradaic – charge transferred across the electrified interface as a result of an electrochemical reaction.
2. Non-Faradaic – charge associated with the movement of electrolyte ions, reorientation of solvent dipoles, adsorption/desorption, *etc.* at the electrode–electrolyte interface. This is the background current in voltammetric measurements.

The interface between electrode and electrolyte is of key importance and this has been considered in detail over the years. The structure of the electric double layer is based on the interfacial characteristic of the electrode, that is, the excess electronic charge at the metal surface, and on the charge-compensating ions in the electrolyte, and well described in the Bockris–Devanathan–Müller model,[1] which brings together inner and outer Helmholtz planes at the metal–electrolyte interface with a diffuse surrounding layer, Figure 13.1.

The Butler–Volmer equation is describes how the electrical current at an electrode depends on the electrode potential, and it is valid where the electrode transfer is dominated by charge transfer as opposed to diffusion; however, it has wide utility in understanding electrode kinetics.

$$i \quad i_0 \cdot \left[\exp\left(\frac{\alpha_A nF}{RT}\eta\right) - \exp\left(-\frac{\alpha_C nF}{RT}\eta\right)\right] \tag{13.6}$$

where i: electrode current density, A m^{-2} : i_0: exchange current density, A m^{-2} , T: absolute temperature, K, n: number of electrons involved in the electrode reaction, F: Faraday constant, R: universal gas constant, α_C: so-called cathodic charge transfer coefficient, dimensionless, α_A: so-called anodic charge transfer coefficient, dimensionless, η: activation overpotential (defined as the electrode potential minus the equilibrium potential, V), see Figure 13.2.

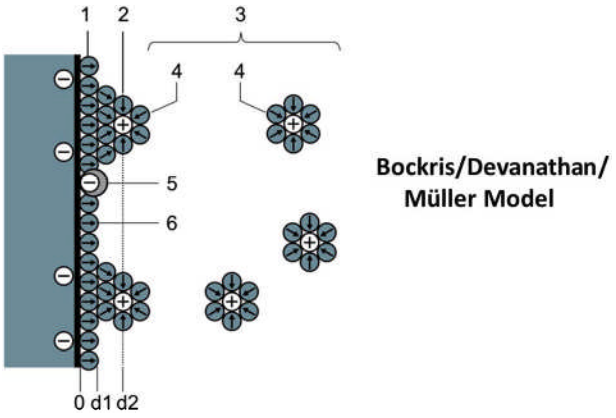

Figure 13.1 Bockris–Devanathan–Müller model. Schematic representation of a double layer on an electrode. 1. Inner Helmholtz plane (IHP); 2. Outer Helmholtz plane (OHP); 3. Diffuse layer; 4. Solvated ions (cations); 5. Specifically adsorbed ions (redox ions, which contribute to the pseudocapacitance); 6. Molecules of the electrolyte solvent.

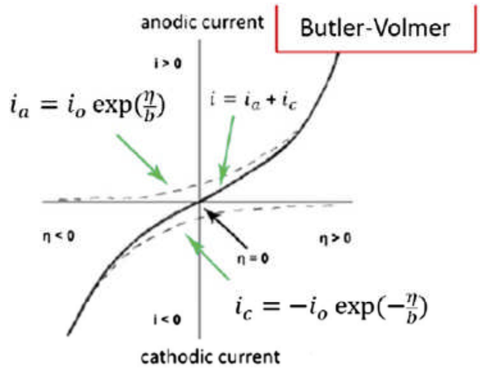

Figure 13.2 Butler–Volmer relation. The graph shows the current as a function of the overpotential η. The anodic and cathodic current densities are shown as i_a and i_c.

13.1.3 Electrocatalysis

A catalyst is defined as a substance that can alter the velocity of a certain chemical reaction without any chemical change, hence an electrocatalyst is an electrode material that interacts with certain species during a Faradaic reaction but still remains unaltered. Since electrode reactions are heterogeneous, electrocatalysts are usually heterogeneous catalysts, which means that the reactions take place on the surface of the catalysts, and there exist adsorption/desorption steps on the surface of the electrocatalysts. In order to compare the catalytic activity of different electrode materials, one can compare the current density at a constant overpotential, or measure the overpotential at a constant current density. A good electrocatalyst should show high current density at low overpotential.

The Sabatier Principle states that, in order to have high catalytic activity, the interaction between reactants and catalysts should neither be too strong nor too weak. If the interaction is too weak, then there will be no reaction on the surface because it is difficult for the catalyst surface to bind the reactants. If the interaction is too strong, then it is difficult for the reactant or product to desorb from the catalyst surface, which also lowers the activity. This principle also applies to electrocatalysis, basically 'some' adsorption is favoured, but not too much. The Sabatier principle usually gives rise to so-called volcano plots, as first introduced by Balandin in 1969.[2]

13.2 Electrocatalytic Production of Ammonia

The electrosynthesis of ammonia is an alternative to the Haber–Bosch process that may prove to offer higher efficiency for the small to medium scale production of ammonia utilising renewable electricity. The various approaches provide a useful window to consider different exemplifications of electrocatalysis for the purposes of this chapter. Ammonia has been synthesised electrochemically in various types of electrochemical cells, which have been mainly classified by the type of electrolyte, such as liquid electrolyte, molten salt, composite membrane and solid electrolyte. Liquid electrolytes consist of ionic salts dissolved in diluted acid solutions,[3] ionic liquids[4] or organic solvents. The advantage of liquid electrolytes is that the reaction can be carried out at room temperature; however, the presence of water in the electrolyte affects the ammonia formation rate, although non-aqueous solvents offer lower solubility. Molten ionic salts offer a more practical operating temperature of 300–500 °C.[5] The molten ionic salt is usually prepared and kept under inert atmosphere, which makes these less practical for industrial purposes. Therefore, solid electrolytes seem to have advantages over other types of electrolytes. The membrane of a solid electrolyte is easy to handle and scalable. Moreover, the solubility and reaction of the produced ammonia in the liquid phase electrolyte are eliminated. Similarly to a membrane reactor, solid membrane electrolytes also work as gas separators. Only reactive ions (such as H^+) involved in the reaction can transport through the solid electrolyte. For ammonia synthesis, a membrane reactor with a proton conducting membrane as the electrolyte is practically employed, the so-called Proton Conducting Membrane Reactor (PCMR). The electrolyte materials for PCMR can be either ceramics or polymers.

Electrochemical processes offer the possibility to produce ammonia under milder working conditions than those of the Haber–Bosch process. Ammonia can be electrochemically synthesised under atmospheric pressure without thermodynamic limitation. As mentioned before, the ammonia industry depends very much on natural gas and consequently releases huge amounts of CO_2.

In general, a solid-state electrocatalytic membrane reactor consists of a dense membrane electrolyte, a porous anode and a porous cathode. The general requirements for the membrane reactor are the same as those for typical solid-state fuel cells and are as follows:

- The electrolyte membrane should be dense, crack-free and gas-tight. The ionic conductivity of the electrolyte should be in the range of 10^{-2} S cm^{-1} with negligible electronic conduction under operating conditions. The electrolyte membrane must be chemically stable under both anode and cathode atmosphere.
- The electrolyte membrane should be thin in order to minimise the ohmic resistance. The mechanical strength of the thin membrane must be reasonable.
- The electrode should have adequate porosity and suitable pore size. The electronic conductivity of the electrode should not be less than 10 S cm^{-1} under the operating atmosphere. The chemical stability of the material under the operating atmosphere must be reasonable.
- The thermal expansion coefficient between the two electrodes and the electrolyte must be matched in order to ensure the transportation of ions at the electrode–electrolyte interface.
- The electrode material must have good catalytic activity. Detailed information on each electrode reaction can be found in the following section.

Basically, solid-state membrane materials are classified by the type of ions conducted. So far, there are two types of solid-state membranes that have been used for ammonia synthesis, proton and oxide ion-conducting membranes. In those membrane reactors, the operating principles are slightly different, as depicted in Figure 13.3.

An oxide ion membrane was firstly utilised for ammonia synthesis by Skodra and Stoukides.[7] A ceramic membrane of yttria-stabilised zirconia with Ru-based electrodes was utilised; however, the ammonia formation rate was quite low. The main disadvantage of this oxide ion membrane reactor is the inconvenient stepwise process for separating the ammonia produced from the residual steam. Proton conducting membranes provide more flexible choices of reactants, varying from hydrogen or water to natural gas and some gaseous hydrocarbons. According to the operating principle, protons generated at the anode from any hydrogen source will be electrochemically transferred through the membrane to react with nitrogen at the anode. The produced ammonia is easily separated from gaseous nitrogen by a condensation unit. Hence, proton conducting membrane reactors seem to be promising reactors for industrial ammonia synthesis.

For the synthesis of ammonia, gaseous hydrogen or water is fed into the anode chamber, where gaseous nitrogen is flowed into the cathode chamber. When a current is imposed through the cell by an external power source, the protons from the anode are pumped through the membrane to the cathode. The emerged protons at the cathode should react with gaseous nitrogen forming ammonia. The transported protons of electrochemical h

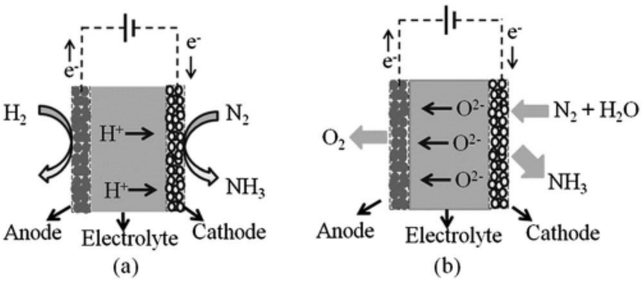

Figure 13.3 Schematic illustration of the operating principles in solid state membrane reactors: (a) proton conducting membrane, and (b) oxide-ion membrane. Figure reprinted from *Membrane Reactors for Energy Applications and Basic Chemical Production*, Membrane reactors for ammonia production, S. Klinsiruk *et al.*, 543–563, Copyright 2015 with permission from Elsevier (adapted from ref. 6).

one of the reactants in the reaction. Hence, the current efficiency is evaluated by Faraday's Law.

$$\Lambda = \Delta r/(I/nF) \tag{13.7}$$

Λ is the rate enhancement factor and Δr is the rate of hydrogen consumption at the cathode. I/nF is the rate of hydrogen flux transported through the membrane, where I is the imposed current, F is Faraday's constant, and the number of moles of electrons involved in the hydrogen oxidation (n) is equal to 2. If all the pumped protons are consumed at the cathode, Λ is equal to 1, which is called Faradaic efficiency.[8] Figure 13.4 illustrates a single-chamber reactor, where reactant gases are mixed and directly fed into the same chamber.

In a single-chamber reactor, the Λ value can exceed the unity as additional hydrogen from the gas phase complements the electrochemical h lled non-Faradaic Electrochemical Modification of the Catalytic Activity (NEMCA). The concept of the NEMCA effect is quite different from that of the Faradaic effect. In NEMCA, an electrode will serve as catalyst for two simultaneous processes, chemical and electrochemical.

Without a current, ammonia can be produced catalytically at the electrocatalyst as a *non-Faradaic* product. When imposing a current, the catalytic activity of the electrocatalyst will be modified by the electrochemical spillover of ions from the membrane electrolyte to the electrocatalyst surface, resulting in a new formation rate achieved from both catalytic and electrocatalytic reactions.[9] Though this type of reactor may provide a higher ammonia formation rate, the separation of the produced ammonia from the non-utilised reactants may be inconvenient, especially when using water as a reactant.

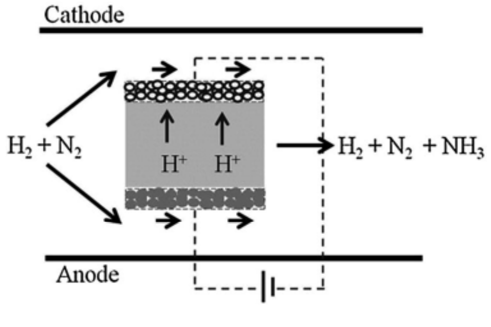

Figure 13.4 Schematic diagram of a single-chamber reactor for ammonia production. Reprinted from *Membrane Reactors for Energy Applications and Basic Chemical Production*, Membrane reactors for ammonia production, S. Klinsiruk *et al.*, 543–563, Copyright 2015 with permission from Elsevier.

When using hydrogen and nitrogen as the reactants, the hydrogen oxidation reaction readily occurs at the anode and the ammonia is evolved at the cathode. At the anode,

$$H_2 \rightarrow 2H^+ + 2e^- \qquad (13.8)$$

Then, the protons are transported through the proton conducting membrane to the cathode, with the flux relating to the imposed current or potential. The resultant protons at the cathode then react with N_2 to form ammonia.

$$3H^+ + 1/2N_2 + 3e^- \rightarrow NH_3 \qquad (13.9)$$

The overall reaction is

$$3H_2 + N_2 \rightarrow 2NH_3 \qquad (13.10)$$

Thermodynamically, this reaction is non-spontaneous with a reaction Gibbs energy ($\Delta_r G^0$) > 0 at temperatures above 130 °C; therefore, this reaction needs to be done under electrolysis conditions.

In some cases, it is possible to observe small amounts of ammonia before imposing a potential. It is likely that the reaction occurs due to a difference in the chemical potentials of the electro-active ionic species (in this case protons) between the two electrodes, which induces some of the protons to move from the anode (higher concentration) to the cathode (lower concentration). Theoretically, the reaction at the cathode should not be completed, since transportation of electrons through the electrolyte should be negligibly small and the high resistance external source connected to the electrodes also forbids the flow of electrons. In some electrolyte materials, the presence of electron transport will cause the formation of ammonia at the cathode under open circuit conditions, especially in elevated temperature solid oxide proton conductors. It is important that the desired electrolyte for the membrane reactor has a proton transfer number close to unity, confirming that the electronic conduction is negligible.

Under electrolysis conditions, a constant potential or current will be applied to the membrane cell reactor and drive the reaction forward. Theoretically, the minimum voltage (E) required for the formation of ammonia can be calculated from the correlation with the change in the Gibbs free energy of the reaction ($\Delta_r G$).

$$\Delta_r G = -nFE \qquad (13.11)$$

However, Murakami has suggested that the ammonia synthesis rate may not depend only on the electrolysis potential.[5] Other factors, such as the catalytic activity of the electrode material, the partial pressure of the gaseous reactants and the temperature, are crucial parameters for the kinetics of ammonia synthesis.[7,10]

13.3 Oxygen Electrodes in Solid Oxide Cells

The electrocatalytic reduction and evolution of molecular oxygen are critical electrochemical reactions in many processes. In the oxygen reduction reaction (ORR), the oxygen molecule combines with electrons to form a product, whereas the oxygen evolution reaction (OER) generates O_2 molecules by taking electrons away from a reactant. Oxygen electrochemistry is at the heart of several renewable energy technologies such as water electrolysis, metal–air batteries, fuel cells and other industrial applications, as suitably illustrated in Figure 13.5.

One exemplar oxygen electrochemical process is oxygen reduction in a Solid Oxide Fuel Cell (SOFC). The overall electrochemical reaction that is promoted at the cathode is the reduction of oxygen:

$$\frac{1}{2}O_2 + V_0^{\bullet\bullet} + 2e' \rightarrow O_0^x \tag{13.12}$$

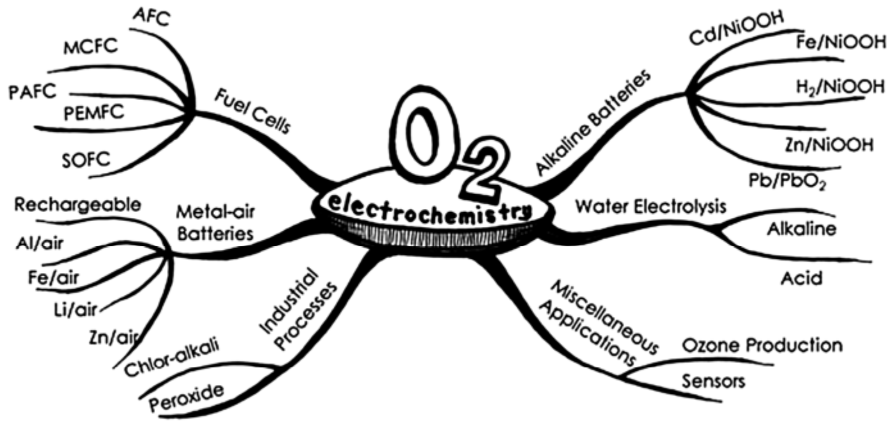

Figure 13.5 Mind map of oxygen electrochemical technologies and processes where O_2 electrochemistry plays a vital role. Reprinted from *Current Applied Physics*, **13**, Oxygen electrocatalysis in chemical energy conversion and storage technologies, 309–321, Copyright 2013 with permission from Elsevier.[11]

From prior studies on cathodes, it seems that there are two distinct types of behaviour:

i. Triple phase boundary (tpb) t le of the oxide material is as an electronic conductor and the oxygen reduction reaction takes place at the cathode–electrolyte–gas phase boundary. For this type of electrode, it is very important to optimise the microstructure to maximise the tpb length per unit area of the cathode. This type of cathode is also very prone to contamination by impurities.
ii. Mixed Ion and Electron Conductors (MIECs). Here, the oxygen reduction is extended over part of the surface of the cathode material and, hence, superior performance can be obtained especially at low temperatures. This makes MIECs the preferred type of cathode for the development of Intermediate Temperature SOFCs (ITSOFCs). For this type of material is an understanding of the kinetics of oxygen exchange and diffusion in these mixed conducting materials.

Perovskite oxides have been employed as fuel cell cathodes for many years. The most well-known ones are materials from the family $(La_{1-x}Sr_x)_{1-y}MnO_3$, commonly abbreviated as LSM. These materials were used as early cathodes on the first zirconia-based high temperature SOFCs and are still the main commercial material. The LSM family behave as tpb cathodes owing to their low diffusivity towards oxygen.[12]

Most of the best perovskite cathodes, particularly for ITSOFC operation, have Co on the B site and a high degree of non-stoichiometry. An example would be the material $Sm_{0.5}Sr_{0.5}CoO_{3-\delta}$; unfortunately, these materials have two drawbacks: they tend to react with yttria-stabilised zirconia (YSZ), the most commonly used electrolyte material, and they suffer from very high expansion coefficients as a result of the chemical expansion component to the thermal expansively. Ullmann *et al.*[13] reported that the expansion coefficient of these materials correlates very well with the oxygen ion conductivity (and hence the diffusivity) of these materials at 800 °C, with the best mixed conducting materials showing some of the highest expansion coefficients ($20–30 \times 10^{-6}\ K^{-1}$).

There are a number of models suggested for SOFC cathode behaviour.[14–17] For cathode materials for application in ITSOFCs, the focus is essentially on MIEC-t ls. The model developed by Adler, Lane and Steele (ALS) specifically to reproduce the behaviour of a porous MIEC cathode contains both microstructural features and the kinetics of oxygen exchange and diffusion,[17] and is particularly relevant for ITSOFC cathodes. The model includes all aspects of cathode operation but is concerned principally with the chemical exchange of oxygen across the gas solid interface. This phenomenon enters the expression for the cathodic area specific resistance *via* the equation for the chemical resistance of the electrode, R_{chem}.

$$R_{\text{chem}} = \frac{RT}{2F^2}\sqrt{\frac{\tau}{(1-\varepsilon)aC_0^2Dk}}\,\Omega\,\text{cm}^{-2} \tag{13.13}$$

The microstructural parameters τ, ε and a represent the tortuosity, porosity and the surface area of the pores in the cathode. The materials specific parameters are the oxygen self-diffusion and exchange coefficient, D and k, and the density of the oxygen sites in the material C_0; however, C_0 can be considered to be more or less constant for the perovskite and perovskite-related materials generally considered here. It can be seen that the kinetic variables are critical and that they enter the expression as the product of the oxygen self-diffusion coefficient and the surface exchange coefficient, Dk. Using suitable choices for the numerical values of the microstructural variables allows the estimation of the kinetic parameters needed to give low values of the ASR at low temperatures. For example, achieving ~0.1 $\Omega\,\text{cm}^{-2}$ at ~500 °C requires values of the Dk product > ~10^{-14} $\text{cm}^3\,\text{s}^{-2}$. These are high values to attain, particularly at the low temperatures envisaged for the operation of ITSOFCs. As an example, at 500 °C, the Dk value for a $La_{0.6}Sr_{0.4}Co_{0.2}Fe_{0.8}O_{3-\delta}$ (LSCF), the perovskite cathode commonly used at low temperatures, is approximately 10^{-19} $\text{cm}^3\,\text{s}^{-2}$, five orders too low; hence, the need for new materials.

13.4 Electrodes in Low-Temperature Fuel Cells

Proton exchange membrane fuel cells (PEMFCs) are composed of an ion exchange membrane sandwiched between two electrodes. Various proton conducting polymers have been fabricated as electrolytes in PEMFCs such as Nafion and SPEEK. Water management in these systems is crucial since ion exchange membranes rely on water to be conductive but electrodes prefer relatively 'dry' conditions to avoid fuel starvation. A typical working temperature for PEMFCs is around 80 °C and this could be increased to 120 °C at high pressure; this is mainly limited by the water balance in the membrane and electrodes. Noble metals such as platinum are used as electrocatalysts due to their high catalytic activation at low temperatures and high purity hydrogen is chosen as fuel. Impurities such as H_2S and CO are detrimental to platinum catalysts and would lead to a marked degradation of the fuel cell performance. This is due to the poisoning effect of CO to Pt, as CO is more stably absorbed on the Pt surface than H_2 at low temperatures. The main challenges for PEMFCs are the high catalyst loading (Pt on anodes and cathodes), the requirements for cooling and the impurity tolerance. Recent work has mainly focused on developing high temperature ion exchange membranes so that fuel cells could be operated at higher temperatures. This gives the benefit of decreasing or even replacing the loading of noble metals and enables the fuel cells to be thermally self-sustainable, avoiding the requirement of cooling and purifying systems.

Phosphoric acid fuel cells (PAFCs) were the first commercial and widely used fuel cell type. Hydrogen or a hydrogen rich gas mixture is used as fuel. The electrolyte, primarily composed of phosphoric acid (H_3PO_4), is a pure proton conductor with good thermal, chemical and electrochemical stability. The operating temperature of PAFCs is typically between 150–200 °C, which is a compromise between the electrolyte conductivity (increases with the temperature) and the cell life (decreases with the temperature).[18] The electrolyte, however, is highly corrosive and so, only noble metals such as Pt can be used. The large capital cost of PAFCs was improved when Pt/carbon or graphite electrodes were deployed in the 1960s.[19] Over the last 40 years, the fuel electrode in PAFCs has evolved from PTFE-bonded Pt back to PTFE bonded Pt/C, with loadings of Pt decreasing 100-fold to 0.1 mg Pt cm^{-2}. In the same period, the air electrode has similarly changed in composition with loadings decreasing 50-fold to 0.5 mg Pt cm^{-2}. One of the major problems in such fuel cells is the accelerated carbon corrosion and Pt dissolution when cell voltages are above 0.8 V. Therefore, long hot idles at open circuit must be avoided. Another problem usually encountered is electrode flooding and drying, and this has been recognised as one of the major causes of declining fuel cell performance.

13.5 Fuel Electrodes in Solid Oxide Fuel Cells

While there are many different designs of SOFCs that operate at a variety of temperatures, they run above several hundred degrees Celsius and, being made of ceramics, have normally been produced at even higher temperatures. Therefore, all of the components in an anode must be both physically and chemically stable for short times at manufacturing temperatures, and for long times (thousands of hours) at operating temperatures. It is often difficult to observe small, slow degradation mechanisms as they require very long test times.

The anode is not a standalone component and must also be both physically and chemically compatible with the other components of the cell, especially the electrolyte, and interconnect the two other components the anode is in contact with. The thermal expansion of the anode must match that of the other cell components, with no phase changes with significant volume changes, which would cause cracking of the cell upon thermal cycling. Typically, the thermal expansion coefficient (TEC) is about 10–12 ppm $°C^{-1}$ to match that of the electrolyte, but can be varied a bit depending on the design of the cell. The use of composite anodes can allow for adjustment of the TEC for a better match.

Anode materials must also not react with the other cell components at operating temperatures, at least to form deleterious phases. Again, it is the very long operating times at high temperatures that can slowly form blocking phases that slowly degrade the cell/stack performance. Any materials used in an anode must be stable under a wide range of reducing conditions, depending on the load and fuel, at the operating temperature. The anode also experiences a significant range of pO_2 during operation, with very low pO_2 under low loads or at the fuel input, with the pO_2 rising as the fuel is used up under high load or near the outlet of the anode. This increasing pO_2 is compounded by the extra water added to the fuel stream for oxide ion conductors. It is also quite likely over the lifetime of any SOFC system that it will be exposed to air several times while still hot, and so will need to withstand this oxidation. Also for practical and cost reasons, the anode will usually be sintered in air, and so must be stable enough to be fabricated into a device. The best solution to all these problems is to make a material that is stable under both oxidising and reducing conditions.

In its simplest case, the overall reaction in a fuel cell is hydrogen combining with oxygen to give water, but the exact reaction at each electrode and the direction of ion movement depends on whether the electrolyte is a protonic or oxide ion conductor. With a proton conducting electrolyte, H^+ are transported across the electrolyte and react with O_2 on the cathode side. With an oxide ion-conducting electrolyte, O^{2-} ions arrive from the electrolyte and react with H^+ on the surface. Note that, for this oxide ion case, as well as depleting the H_2 from the fuel stream, the product (H_2O) is added to the fuel stream, diluting it further and lowering the pO_2 of the system (Figure 13.6).

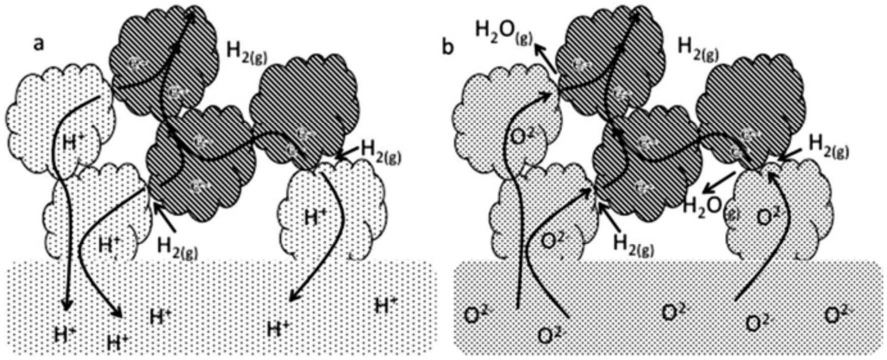

Figure 13.6 Schematic of hydrogen oxidation processes at composite electrodes with (a) proton and (b) oxide ion-conducting electrolytes. Reproduced from ref. 32 with permission from the Royal Society of Chemistry.

The catalytic properties of the anode in a SOFC are very important in determining the overall cell performance. Usually, the catalyst is one of the parts of the anode, and the high temperature gives sufficient kinetics. However, as when using a composite electrode to gain both electronic and ionic conductivity, a small amount of catalyst may be added to the surface of the anode after it has been sintered, *via* impregnation for instance, to improve the electrode behaviour. This places the catalyst more at the triple phase boundary where it is needed and less in the bulk, and so it can be used at much lower loadings to get the same effect as if a much larger amount was used as a component of the anode, which allows the use of more expensive catalyst materials.

Many materials are good at catalysing the oxidation of H_2, such as Pt, Ni and various transition metal oxides. If one of the more commonly available hydrocarbon fuels is to be used in a fuel cell, then the catalyst requirements are more complicated. The catalyst must be able to cope with the oxidation of the hydrocarbon and the higher levels of impurities found in these fuels. In order to use a hydrocarbon directly in a fuel cell, the anode catalyst must be able to oxidise the hydrocarbons, sometimes without the need of water or reforming.[20]

$$CH_{4(g)} + 4O_{(i)}^{2-} \rightarrow CO_{2(g)} + 2H_2O_{(g)} + 8e^- \qquad (13.14)$$

However, this reaction is kinetically slow and so, the hydrocarbons are typically reformed to form smaller molecules, ideall

ly needs to oxidise these species. The reforming can be done externally or *via* internal reforming in the cells themselves reducing the external part count. Hydrocarbons are typically reformed with steam (reaction (13.15)), but can also be reformed with small amounts of O_2/air.

$$CH_{4(g)} + H_2O_{(g)} \leftrightarrow CO_{(g} \qquad _{(g} \tag{13.15}$$

This reaction is endothermic and so enables good synergy to use the waste heat from the fuel cell to drive the reformation. Both the CO and H_2 produced from reforming can be used in an SOFC (unlike low temperature fuel cells), but the anode needs to catalyse the oxidation of both H_2 and CO to CO_2.

$$CO_{(g)} + O_{(i)}{}^{2-} \rightarrow CO_{2(g)} + 2e^- \tag{13.16}$$

The kinetics of reaction (13.16) are typically more sluggish than the hydrogen oxidation reaction[21] and, in a lot of cases, is bypassed by the faster gas phase water–gas shift reaction (WGSR, reaction (13.17)), reacting the CO with water, from feed or hydrogen oxidation, to form more H_2, which is then utilised by the faster hydrogen oxidation reaction.

$$CO_{(g)} + H_2O_{(g)} \leftrightarrow CO_{2(g} \qquad _{(g)} \tag{13.17}$$

In practice, hydrocarbon fuels are normally introduced with extra water (usually with a minimum steam to carbon ratio of two) over a steam reforming catalyst where reactions (13.4) and (13.6) take place.[22] This situation, where the reforming reactions take place in the outer anode support and with only reformate products reaching the triple phase boundaries, is better described as a direct utilisation rather than direct oxidation.[23] The case where the process is enhanced when the products of the fuel cell reaction are also utilised to drive the reforming process is known as gradual internal reforming (Figure 13.7).[24]

Care needs to be taken in the design and control of the fuel mixture to ensure the speed of the endothermic reformation reactions does not lead to localised cooling of the inlet of the cell, which in turn can create thermal and mechanical stresses that can lead to cracking and failure.[25] The reforming reactions compete with the Boudouard and cracking reactions ((13.18) and (13.19), respectively).

$$CH_{4(g)} \rightleftharpoons C_{(s)} + 2H_{2(g)} \tag{13.18}$$

$$2CO_{(g} \rightarrow CO_{2(g)} + C_{(s)} \tag{13.19}$$

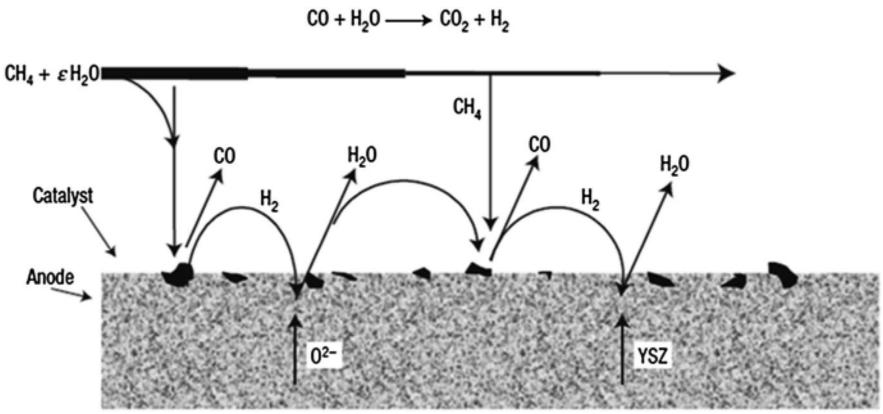

Figure 13.7 The concept of gradual internal reforming of methane introduced by Vernoux and Kleitz.

This formation of solid carbon can quickly block pipes and destroy an anode by filling up the pores and breaking up the structure of the anode. This is a particular problem for Ni-based anodes.

External reforming in a dedicated external unit can allow better control of the reforming process.[26] The heat from the cell stack can be used to maintain the reformer temperature while providing advantageous heat management in the stacks.[27] These external reformers also allow the careful management of the carbon to steam ratio, to ensure no carbon formation anywhere in the system.

The actual details of the process happening in SOFC anodes are not well understood. Many *in situ* spectroscopic probes such as Raman and infrared spectroscopy are routinely used in catalysis research to characterise surface intermediates and reaction mechanisms. It is very difficult, however, to apply these techniques to an operating SOFC anode. Nonetheless, some inroads are being made in this area. For example, Liu and co-workers[28] pioneered the application of infrared emission spectroscopy to characterise working SOFC anodes. The development of models of anodes that allow other spectroscopic probes, such as photoelectron spectroscopy, and detailed kinetic measurements is also needed in order to advance research in this area.

Sulphur compounds are present in many real world fuels, either as a natural impurity such as biogas, diesel and coal gas, sometimes at significant levels, or introduced as a deliberate additive, such as odorants in natural gas supplies for leak detection. Due to the operational temperatures employed in SOFCs, most sulphur compounds will be converted to H_2S by the time they reach either the support or the anode itself. H_2S will react rapidly with the electrode surface, even at ppm levels, to block reaction sites for both steam reforming and fuel oxidation and severely degrading the Ni catalyst performance.[29] Degradation is often a two stage process with an instantaneous drop followed by a slower longer term continuous degradation.[30] While exact mechanisms are still under discussion, it is thought that the main source of the blocking is the formation of sulphides on the surface of the metal.[31] It has also been observed that, while some recovery will take place after removal of the sulphur, there is often a permanent drop in performance, the anode does not fully recover and, in many circumstances, this can be fatal to the operation of a large stack or system. The above paragraphs have provided an outline of some of the issues that Ni-based anodes can face. A more detailed discussion of these issues and the application of fuels beyond hydrogen has been described elsewhere.[32]

13.6 Nanostructure of Electrocatalysts in Solid Oxide Cells

Solid oxide electrolytes are the basis of two important energy technologies, Solid Oxide Fuel Cells (SOFCs) and Solid Oxide Electrolyser Cells (SOECs), which are jointly referred to as Solid Oxide Cells. SOFCs offer efficient alternatives for electricity production and, similarly . These technologies are very flexible with a wide-ranging scale of applications. When practical fuels are used, the environmental impact is better than for combustion technologies with less CO_2 and NO_x produced per unit of power generated. The high quality exhaust heat released during operation can be used as a valuable energy source, *e.g.* to drive a gas turbine when pressurised or to achieve highly efficient electrical-to-chemical conversion.

For a given electrolyte material and thickness, performance is largely determined by the electrode processes and these can be subdivided into Faradaic (largely charge transfer) and non-Faradaic (largely mass transport) processes. The non-Faradaic processes are strongly dependent upon the macroscopic and microscopic features of the electrode as a whole (Figure 13.8), whereas the Faradaic processes are very much dependent upon the nanoscale features of the

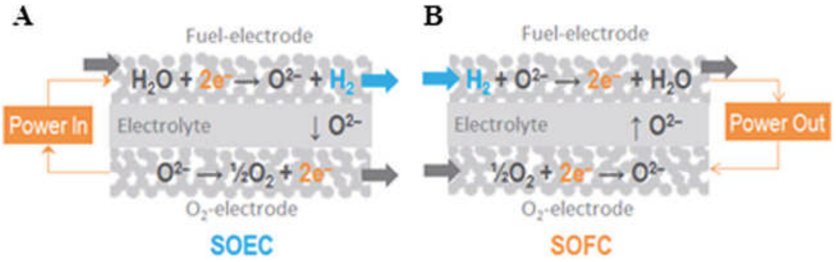

Figure 13.8 Solid Oxide Cell schematics. (A) SOC operating in electrolysis mode, splitting H_2O (or CO_2) electrochemically into H_2 (or CO) and O_2. (B) SOC operating in fuel cell mode; a fuel, for example H_2, is combined electrochemically with O_2 to produce power. SOCs consist of three main components: two porous electrodes, the H_2 (or fuel) and O_2 (or air) electrodes, separated by a dense electrolyte. Simplified electrode reactions are shown for both the SOEC and SOFC modes.[33]

interface between the electrode and electrolyte. This region, which typically only extends a few microns from the electrolyte, is often considered the ‘true electrode’, with the remainder of the electrode having mechanical, electron and gas transport functions.[33] The components, structure and evolution of this interface are central to many of the recent exciting advances in the development and understanding of SOC devices.

A wide range of materials functions and architectures can be implemented to enhance the activity of this electrode/electrolyte interface and its electrochemistry. An ideal cell microstructure would offer optimised contact between the electrolyte and the electrode, while being dimensionally, mechanically, chemically and thermally stable during operation. The electrochemically active region of a SOC electrode must support three essential functionalities that allow for electrochemical reactions to occur effectively. As indicated in Figure 13.9a, these are: high electrocatalytic activity towards desirable reactions such as H_2O splitting or O_2 reduction, ionic conduction (IC) and electronic conduction (EC). Often, the latter are provided from a single material, such as a MIEC. Since electrode reactions occur exclusively at discreet locations where these functionalities converge in the presence of reactants, these locations also constitute the active areas within the electrode structure. Electrodes must be designed with an extended active surface area through the adequate choice of materials, microstructures and porosity, as illustrated in Figure 13.9. For example, for composite electrodes consisting of EC and IC phases, the active

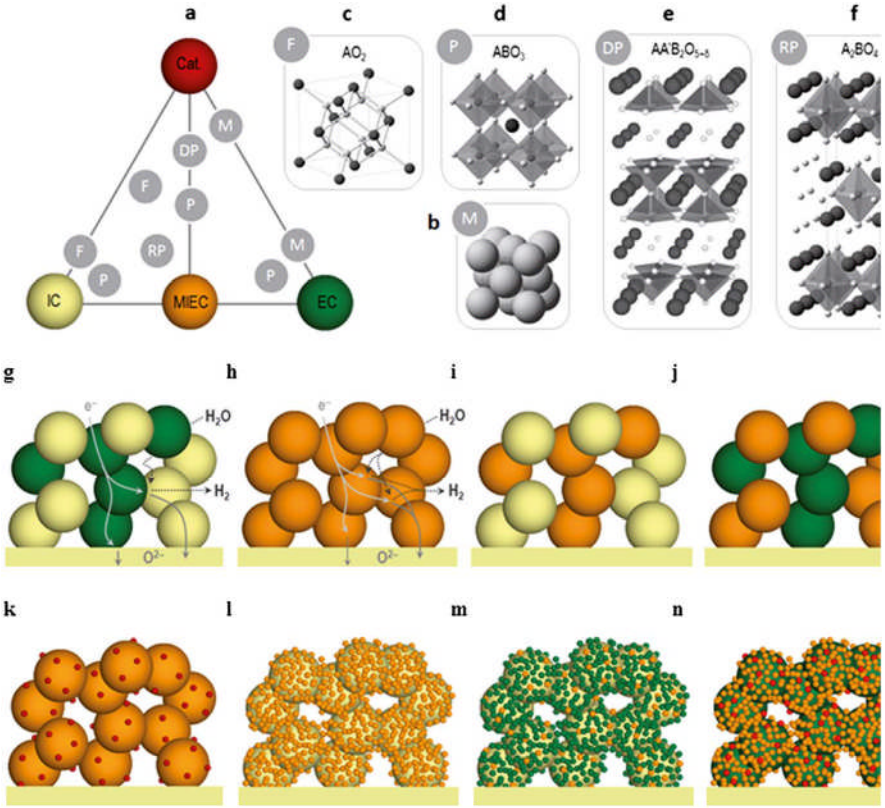

Figure 13.9 Materials and microstructures for SOC electrodes. (a) Diagram highlighting the three key functionalities that electrodes should exhibit to operate effectively (vertices) and the classes of materials employed to deliver this (marked circles). Functionalities include: ion conduction (IC), electron conduction (EC), or combined mixed ion and electron conduction (MIEC), and catalytic activity for desirable reactions (Cat.; *e.g.* water splitting). (b) Crystal structure of a metal (Ni), which excels at electronic conductivity and catalysis. (c) Fluorite crystal structure, which excels at ionic and catalytic functions. (d) Perovskite crystal structure, which exhibits all types of functionality to various extents, although it does not always excel in terms of catalysis. (e) Crystal structure of oxygen deficient, layered perovskites, which are close to being the ideal single-phase electrode material as they exhibit the full range of desirable functionalities. (f) Crystal structure of a member of the Ruddlesden–Popper phase, a perovskite-related structure associated with high interstitial oxygen diffusion rates. (g–n) Schematic illustrations of electrodes highlighting the key types of microstructures and classes of functional materials used to build them (see (a) for colour coding). (g) IC–EC composite structure; also illustrates a 3PB fuel-electrode in SOEC mode. (h) Single-phase MIEC electrode; also illustrates a 2PB fuel-electrode in SOEC mode. (i) IC–MIEC composite structure. (j) MIEC–EC composite structure. (k) MIEC with dispersed catalyst particles. (l) IC coated with a percolating layer of MIEC. (m) IC coated with a percolating layer of EC and MIEC. (n) EC coated with a percolating layer of MIEC and dispersed catalyst.[33]

areas are located exclusively at the interface between the EC, IC and gas phases, as illustrated in Figure 13.9g; hence, these are referred to as three phase boundary (3PB) points. If the electrode is a MIEC, then the entire electrode surface exposed to the reacting gas might in principle be active towards electrochemical reactions (see Figure 13.9h); the reactions take place at the solid–gas two phase boundary (2PB). Other, more elaborate electrode microstructures may be used to maximise 3PB and/or 2PB regions, as shown in Figure 13.9l–n, by selecting dedicated materials to fulfil the desired functions (Figure 13.9a).[33]

Acknowledgements

The author would like to thank his colleagues (Dr M. Cassidy, Dr S. Klinsrisuk, Prof. S. W. T . X. X. Xu, Dr D. Neagu, Prof. J. Kilner, Prof. M. Mogensen) for their contribution to various articles that are brought together in this chapter.

References

1. J. O'M. Bockris, M. A. V. Devanathan and K. Muller, *Proc. R. Soc. A*, 1963, **274**, 55.
2. A. A. Balandin, *Adv. Catal.*, 1969, **1**, 19.
3. F. Köleli, D. Röpke, R. Aydin and T. Röpke, *J. Appl. Electrochem.*, 2011, **41**(4), 405.
4. T. M. Pappenfus, K. M. Lee, L. M. Thoma and C. R. Dukart, *ECS Trans.*, 2009, **16**, 89.
5. T. Murakami, T. Nishikiori, T. Nohira and Y. Ito, *J. Electrochem. Soc.*, 2005, **152**(5), D75.
6. I. A. Amar, C. T. G. Petit, L. Zhang, R. Lan, P. J. Skabara and S. W. Tao, *Solid State Ionics*, 2011, **201**, 94.
7. A. Skodra and M. Stoukides, *Solid State Ionics*, 2009, **180**, 1332.
8. C. Kokkofitis, M. Ouzounidou, A. Skodra and M. Stoukides, *Solid State Ionics*, 2007, **178**, 507.
9. N. A. Anastasijevic, *Catal. Today*, 2009, **146**, 308.
10. G. Marnellos, S. Zisekas and M. Stoukides, *J. Catal.*, 2000, **193**, 80.
11. J. Lee, B. Jeong and J. D. Ocon, *Curr. Appl. Phys.*, 2013, **13**, 309.
12. S. Carter, A. Selcuk, R. J. Chater, J. Kajda, J. A. Kilner and B. C. H. Steele, *Solid State Ionics*, 1992, **53–56**, 597.
13. H. Ullmann, N. Trofimenko, F. Tietz, D. Stover and A. Ahmad-Khanlou, *Solid State Ionics*, 2000, **138**, 79.

14. E. Ivers-Tiffee, A. Weber, K. Schmid and V. Krebs, *Solid State Ionics*, 2004, **174**, 223.
15. S. B. Adler, *Chem. Rev.*, 2004, **104**, 4791.
16. A. M. Svensson, S. Sunde and K. Nisancioglu, *Solid State Ionics*, 1996, **86–88**, 1211.
17. S. B. Adler, J. A. Lane and B. C. H. Steele, *J. Electrochem. Soc.*, 1996, **143**, 3554.
18. N. Sammes, R. Bove and K. Stahl, *Curr. Opin. Solid State Mater. Sci.*, 2004, **8**, 372.
19. J. H. Hirschenhofer, D. B. Stauffer, R. R. Engleman and M. G. Klett, *Fuel Cell Handbook*, 4th edn, DOE/FETC-99/1076, 1998.
20. E. S. Hecht, G. K. Gupta, H. Zhu, A. M. Dean, R. J. Kee, L. Maier and O. Deutschmann, *Appl. Catal., A*, 2005, **295**, 40.
21. P. Holtappels, L. G. J. De Haart, U. Stimming, I. C. Vinke and M. Mogensen, *J. Appl. Electrochem.*, 1999, **29**, 561.
22. T. Takeguchi, Y. Kania, T. Yano, R. Kikuchi, K. Eguchi, K. Tsujimoto, Y. Uchida, A. Ueno, K. Omoshiki and M. Aizawa, *J. Power Sources*, 2002, **112**, 588.
23. S. McIntosh and R. J. Gorte, *Chem. Rev.*, 2004, **104**, 4845.
24. P. Vernoux, J. Guindet and M. J. Kleitz, *J. Electrochem. Soc.*, 1998, **145**, 3487.
25. M. Boder and R. Dittmeyer, *J. Power Sources*, 2006, **155**, 13.
26. R. Peters, E. Riesche and P. Cremer, *J. Power Sources*, 2000, **86**, 432.
27. R. Peters, R. Dahl, U. Klüttgen, C. Palm and D. Stolten, *J. Power Sources*, 2002, **106**, 238.
28. X. Y. Lu, P. W. Faguy and M. I. Liu, *J. Electrochem. Soc.*, 2002, **149**(10), A1293.
29. J. Sehested, *Catal. Today*, 2006, **111**, 103.
30. S. Zha, Z. Cheng and M. Lui, *J. Electrochem. Soc.*, 2007, **154**, B201.
31. Z. Cheng and M. Lui, *Solid State Ionics*, 2007, **178**, 925.
32. M. Cassidy, J. P. Ouweltjes and N. Dekker, RSC Energy & Environment Series v2, in *Innovations in Fuel Cell Technologies*, ed. R. Steinberger-Wilkens and W. Lenhart, 2010, pp. 153–189.
33. J. T. S. Irvine, D. Neagu, M. C. Verbraeken, C. Chatzichristodoulou, C. Graves and M. B. Mogensen, *Nat. Energy*, 2016, **1**, 15014.